

# A $^{13}\text{C}(\alpha, \text{n})^{16}\text{O}$ calibration source for KamLAND

David W. McKee, Jerome K. Busenitz <sup>\*</sup>, Igor Ostrovskiy

*University of Alabama*

## Abstract

We report on the construction and performance of a calibration source for KamLAND using the reaction  $^{13}\text{C}(\alpha, \text{n})^{16}\text{O}$  with  $^{210}\text{Po}$  as the alpha progenitor. The source provides a direct measurement of this background reaction in our detector, high energy calibration points for the detector energy scale, and data on quenching of the neutron visible energy in KamLAND scintillator. We also discuss the possibility of using the  $^{13}\text{C}(\alpha, \text{n})^{16}\text{O}$  reaction as a source of tagged slow neutrons.

*Key words:* KamLAND, calibration, source, alpha, carbon-13

*PACS:* 29.25.Dz, 29.40.Mc

## 1. Introduction

The reactor phase of the Kamioka Liquid scintillator Anti-Neutrino Detector (KamLAND) detects the interaction



by observing the delayed coincidence between the positron and the subsequent capture of the neutron.[1] A trigger can be generated by any reaction which produces a prompt signal above threshold and a free neutron.

A particular background in KamLAND results from the presence of  $^{210}\text{Po}$  (a daughter of  $^{222}\text{Rn}$  present in quantities governed by the  $^{210}\text{Pb}$  concentration), which decays by emitting a 5.304 MeV  $\alpha$  particle, allowing the alpha capture reaction



This reaction has been studied since the 1950s, [2,3,4,5] and Harrisopoulos et al. recently measured the cross-section to 4%. [6] However, the current theoretical understanding of the reaction was insufficient to describe the response of KamLAND to the reaction in Eq. 2 due to uncertainties in the neutron spectrum and the poorly known excited state branching fractions.

We have produced and deployed a calibration source utilizing the reaction in Eq. 2 to carry out a direct measurement of the background rate and the energy spectrum for this reaction in KamLAND. Similar sources reported in the extant literature[7,8,9] use different progenitor isotopes and were constructed as gamma calibration sources for germanium detectors; while we are as interested in the neutron as the decay gamma.

## 2. Design and Construction

To obtain an accurate measurement of the prompt neutron energy spectrum in KamLAND requires either  $^{210}\text{Pb}$  or  $^{210}\text{Po}$  as the progenitor—other isotopes generate different alpha energies. Despite

<sup>\*</sup> Department of Physics and Astronomy; University of Alabama; Box 870324; Tuscaloosa, AL 35487

Email addresses: dmckee@bama.ua.edu (David W. McKee), busenitz@bama.ua.edu (Jerome K. Busenitz), iostrovskiy@bama.ua.edu (Igor Ostrovskiy).

the short half-life of the Polonium isotope—138.4 days—we judged it feasible to construct a source, certify it for use in the detector, and deploy it on a time scale comparable with the  $^{210}\text{Po}$  half-life. After our attempts to obtain  $^{210}\text{Pb}$  in sufficient quantities were unsuccessful, we decided to build a source with  $^{210}\text{Po}$ .

The strongest design constraints were imposed by the stringent local regulatory limits on contained activity and the very low capture fraction for alpha particles. We were limited to an initial contained activity of 100  $\mu\text{Ci}$  of  $^{210}\text{Po}$ . Assuming this limit and computing the expected capture fraction (see section 6.3) we could estimate a neutron rate for the source no higher than 30 Hz.

We were able to obtain  $^{210}\text{Po}$  in a 4 M hydrochloric acid solution and high purity  $^{13}\text{C}$  in powder form. The source was constructed by filling the capsule with approximately 0.3 g of  $^{13}\text{C}$  powder, dripping the Polonium solution into the carbon powder, and allowing the whole to dry thoroughly before tamping the powder with a Delrin spacer and closing the system. A heat lamp was used to speed the evaporation, which required two days. Our design called for a total contained activity of 95  $\mu\text{Ci}$  on the day of assembly.

The source capsule—shown in Fig. 1—was constructed of stainless steel for ease of manufacture. The inner capsule was constructed of series 316L stainless steel for acid resistance, and series 304 stainless steel was used in the outer capsule for its good welding properties. Both materials are known to be compatible with KamLAND liquid scintillator (LS).

Despite the use of low carbon stainless steel in the inner capsule, tests showed that it would nonetheless develop gas bubbles in the presence of HCl that threatened to spatter our alpha source around the fume hood. To prevent this, we painted the inside of the capsule with four thin coats of a clear acrylic paint obtained at a local craft store. This treatment provided adequate acid resistance.

The inner capsule was sealed using a structural adhesive,<sup>1</sup> wiped clean, and inserted in the outer capsule, which was welded shut using an electron beam technique.

### 3. Certification

Objects to be deployed in KamLAND must first be certified as both chemically compatible with the LS and radiologically clean. In particular, it is necessary to show that radiological sources are properly sealed and do not leak.

Following standard KamLAND procedure, we thoroughly cleaned the source, and then soaked it in 0.1 M nitric acid for four days, pressure cycling to five atmospheres three times in the course of the soak. The soak liquid was counted in a high sensitivity germanium detector to exclude gamma radio-contamination. Special attention was paid to the possible presence of  $^{40}\text{K}$ , and the daughters of  $^{238}\text{U}$  and  $^{232}\text{Th}$ .

Because  $^{210}\text{Po}$  does not have a significant gamma line, this method is not well suited to detecting a low activity Polonium leak. Instead we introduced a sample of the soak liquid into a cuvet full of acid tolerant liquid scintillator,<sup>2</sup> which was subsequently placed between two PMTs and the signal from any alpha activity observed directly. Understanding this device required calibration data with several gamma sources to establish the energy response; with a clean control sample to understand the shape of the background (mostly cosmic rays and ambient radioactivity); and with a  $^{210}\text{Po}$  doped sample to establish the quenching behavior of the LS. A null result was obtained for measured  $^{210}\text{Po}$  leakage with a 90% C.L. upper limit of 0.3 Bq, and the source was certified for use in KamLAND.

### 4. Source Physics

KamLAND signals from the source arise from three mechanisms: prompt activity from the alpha progenitor, prompt activity from the alpha capture reaction, and delayed activity from the capture of the thermalized neutron.

At the alpha energy of  $^{210}\text{Po}$ , Eq. 2 can proceed not only to the ground state of  $^{16}\text{O}$ , but also to the first two excited states. See Table 1 for thresholds and decay products.

#### 4.1. Progenitor activity

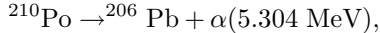
The  $^{210}\text{Po}$  progenitor decays primarily by

---

<sup>1</sup> 3M Scotch Grip 1357

---

<sup>2</sup> Packard Ultima Gold AB



but has a  $(1.21 \pm 0.04) \times 10^{-5}$  branch to



The gamma line proved to be useful for calibrating the total contained activity of the source. See section 6.1.

#### 4.2. Prompt signal

The final state of Eq. 2 contains two particles, either of which can contribute to a prompt detector signal. In practice the visible energy is mainly due to one particle. Captures to the ground state of  $^{16}\text{O}$  result in energetic neutrons which will often generate enough scintillation light to pass the prompt trigger threshold. The neutrons associated with excited state captures are too low in energy to generate a trigger in this way, but the decay products of the excited oxygen nuclei are well above threshold.

The neutrons emitted from captures to the ground state have a broad energy spectrum between approximately 3.0 and 7.3 MeV, peaking near 4.8 MeV. The scattering of fast neutrons off of protons in the liquid scintillator can produce a PMT signal sufficient to develop a prompt trigger without contribution from other mechanisms. Furthermore, a fast neutron can lose a large fraction of its energy in a single inelastic scattering event on carbon by



followed by a prompt decay of the excited carbon nucleus with emission of a 4.4 MeV  $\gamma$ .

#### 4.3. Delayed signal

As in the neutrino events KamLAND was designed to detect, thermalized neutrons are captured primarily by  $^1\text{H}$  or rarely by  $^{12}\text{C}$ . These processes produce signals of 2.2 and 4.95 MeV respectively. The mean neutron capture time in the detector is slightly more than 200  $\mu\text{s}$ .

### 5. Deployment and Data Set

Once the source was certified for use in KamLAND, we deployed it to a number of points along the vertical symmetry axis of the detector in November 2006 and again in March of 2007. The source was

also deployed off the symmetry axis during January 2007. Though some 16 positions along the vertical axis and several off axis geometries were probed, this analysis concerns itself with runs taken at the detector center.

KamLAND triggers are based on the number, NSUM, of PMTs detecting at least one photo-electron and the data acquisition (DAQ) hardware can limit the total DAQ rates by dividing each second into active and inactive windows. We had two separate needs: to accurately measure the contained activity of the device (using the decay gamma line in Eq. 3) and to capture as much data on the prompt and delayed spectra as possible. For the first need we used a simple trigger—denoted the ‘activity’ trigger—which captured 35% of all events with  $\text{NSUM} > 70$  (i.e. with gamma equivalent energy of  $\approx 250$  keV at the detector center). For the second goal we employ the so-called ‘spectrum’ trigger which captures all events with  $\text{NSUM} > 190$  and 1% of all other events down to NSUM of 40.

### 6. Source Performance Analysis

The data from the polonium–carbon source are being used by the KamLAND collaboration to characterize the  $^{13}\text{C}(\alpha, n)^{16}\text{O}$  background to the experiment, to better understand the properties of the KamLAND liquid scintillator, and to tune the performance of our event reconstruction algorithms. Here we present results of an analysis to measure the rates from the source in order to characterize it and demonstrate that it performs as expected.

All analysis includes a geometric cut constraining our consideration to events reconstructed within 120 (150) cm of the source position for prompt events (neutron captures) and a timing cut excluding the 2 ms following the detection of a muon (i.e. a cosmic ray event which swamps the DAQ). These cuts reduce the total data set considerably but retain all source-related events.

Figure 2 displays a singles spectrum after the geometric and muon cuts have been applied. Gaussians have been fit to several of the interesting features of the spectrum.

#### 6.1. Contained $^{210}\text{Po}$ Activity

Measurement of the contained activity consists of fitting a Gaussian plus linear background to the

reconstructed energy near 803 keV in runs using the activity trigger.

Monte Carlo studies indicate that  $15 \pm 1\%$  of events suffer significant scattering losses in the source capsule and are not fit.

The data are sufficient to fit an exponential decay curve as shown in Fig. 3. The fit yields a half-life for the source of  $135 \pm 5$  days—consistent with the accepted value for  $^{210}\text{Po}$ —and gives the initial contained activity as  $3.02 \pm 0.13 \pm 0.10 \text{ MBq} = 81.6 \pm 3.5 \pm 2.7 \mu\text{Ci}$  of  $^{210}\text{Po}$  correcting for the fitting fraction (the first error represents the fitting error for the 803 keV peak including statistics; the second represents the uncertainties of the branching ratio and the fitting losses taken in quadrature). This is in reasonable agreement with the design activity of  $95 \mu\text{Ci}$  taking into account that some loss of activity by adherence to the glassware during fabrication could be expected.

## 6.2. Delayed Coincidence Rate

We find prompt–delayed coincidences by looking for two events separated by less than 1.5 ms and having a reconstructed energy in the later event near 2.2 or 4.95 MeV. In practice, we identify candidate neutron captures first, then work backwards in time searching for corresponding prompt events. A example of the results appears in Fig. 4.

This method is used to select pairs for all subsequent analysis. Further, we associate a weight with each event to correct for the trigger fraction. Monte Carlo simulations of the trigger behavior are used to establish the correct weight for each trigger and NSUM range. We measured delayed coincidence rates of approximately 10 Hz in November 2006 and 5.5 Hz in April 2007. These results do not include the neutrons captured on Fe, Co, Ni in the source capsule and the deployment hardware (totalling a few percent of the rate) nor does it account for the selection efficiency of the analysis ( $\approx 1.5\%$ ). The measured coincidence rates are consistent with the measured  $^{210}\text{Po}$  activity.

## 6.3. Alpha Capture Fraction

Computing the delayed coincidence rate as a function of the contained activity averaged across all runs we find  $(6.1 \pm 0.3)$  events/s/(MBq of  $^{210}\text{Po}$ ). The expected alpha capture fraction from integrating the cross-sections and stopping powers reported

in the literature is  $(7.1 \pm 0.3)$  events/s/(MBq of  $^{210}\text{Po}$ ), neglecting any edge effects in the source capsule and assuming that there has been no formation of Po slugs in the source mixture. We compute the neutron activity on the day of assembly to have been  $18.4 \pm 1.3 \text{ Bq}$ .

## 6.4. Excited State Captures

As seen in Fig. 4, captures to the second excited state are readily identified by the presence of a 6.13 MeV prompt event—these events are well separated from the prompt neutron continuum and there is little contamination of the sample. These events constitute approximately 1% of the total.

Captures to the first excited state can be identified by the 1022 keV prompt signal from annihilation of the positron. These events are harder to separate from the fast neutron continuum, but a useful peak is present with sufficient statistics. This feature of the source spectrum differs from that expected from the extant background in KamLAND because the kinetic energy of the electron positron pair is fully contained inside the source capsule. Roughly 5% of the total rate is associated with these events.

## 6.5. Tagged Slow Neutrons

The presence of a 6.13 MeV gamma in the final state of the alpha capture reaction is a clean and experimentally accessible indication of an excited state capture and is associated with an initial neutron energy below 0.6 MeV (by comparison both  $^{252}\text{Cf}$  and  $^{241}\text{Am}$ –Be sources produce neutrons with average energy well over 1 MeV). We suggest that the  $^{13}\text{C}(\alpha, n)^{16}\text{O}$  reaction is an effective source of tagged slow neutrons and may be useful in the calibration of future reactor neutrino experiments e.g. Double Chooz or Daya Bay.[10,11].

When constructed as a tagged neutron source, an alpha progenitor with a longer half-life than  $^{210}\text{Po}$  is preferable. Isotopes with significant fission rates should be avoided as they introduce unwanted neutron background. Progenitors with significantly higher alpha energies can achieve much higher branching fractions to the second excited state, but also have higher endpoint energies for neutrons emitted from this state—possibly negating the advantage of tagging a ‘slow’ neutron.  $^{210}\text{Pb}$  is a viable choice, but may be difficult to obtain in sufficient quantity.  $^{241}\text{Am}$  is easily obtainable and long-lived

and thus appears to be a useful progenitor, though care must be taken to shield the detector from 59 keV gamma line. Another possibility is  $^{238}\text{Pu}$ .

## 7. Summary

We have constructed a calibration source based on the reaction  $^{13}\text{C}(\alpha, \text{n})^{16}\text{O}$  using  $^{210}\text{Po}$  as the alpha progenitor and successfully deployed it in KamLAND. Both the neutron rate and the 6.13 MeV gamma rate were consistent with our expectations and were sufficient to accumulate useful statistics in a reasonable time.

Data from the source are being employed to reduce the systematic uncertainty associated with the presence of radon decay daughters in the detector. Efforts to use these data to improve KamLAND event reconstruction and shed additional light on the properties of the KamLAND liquid scintillator—neutron quenching and energy scale—are underway.

**Acknowledgments** This work was done as part of our calibration efforts for KamLAND and could not have proceeded without the support of collaboration as a whole. We would particularly like to acknowledge the assistance of Kazumi Tolich in writing and debugging trigger scripts. We are also indebted to Kevin Lesko and Brian Fujikawa for bringing the possibility of building an  $^{13}\text{C}(\alpha, \text{n})^{16}\text{O}$  source for KamLAND to our attention. The  $^{13}\text{C}$  powder used in constructing the source was supplied by Kevin Lesko. Andreas Piepke aided us in developing the source certification procedure. This work was funded by the US Department of Energy.

## References

- [1] T. Araki et al. [KamLAND Collaboration], Phys. Rev. Lett. **94**, 081801 (2005) [arXiv:hep-ex/0406035].
- [2] R. B. Walton, J. D. Clement and F. Boreli, Phys. Rev. **107** 1065 (1957).
- [3] K. K. Sekharan, A. S. Divatia, S. S. Kerekatte, and K. B. Nambiar Phys. Rev. **156** 1187 (1967).
- [4] J. K. Bair and F. X. Haas, Phys. Rev. C **7**, 1356 (1973).
- [5] G. J. H. Jacobs and H. Liskien Ann. Nuc. Energy **10** 541 (1983).
- [6] S. Harissopoulos, H. W. Becker, J. W. Hammer, A. Lagoyannis, C. Rolfs and F. Strieder, Phys. Rev. C **72**, 062801 (2005).
- [7] J. K. Dickens and R. D. Baybarz, Nucl. Instrum. Meth. **85**, 143 (1970).
- [8] K. W. Geiger and L. Van Der Zwan, Nucl. Instrum. Meth. **157**, 199 (1978).
- [9] J. P. Mason, Nucl. Instrum. Meth. A **A241**, 207 (1985).
- [10] F. Ardellier et al. [Double Chooz Collaboration], arXiv:hep-ex/0606025.
- [11] X. Guo et al. [Daya Bay Collaboration], arXiv:hep-ex/0701029.

Table 1

Summary of relevant data for states of  $^{16}\text{O}$ . Threshold represents the minimum alpha kinetic energy needed to excite the state in  $^{13}\text{C}(\alpha, \text{n})^{16}\text{O}$ .

State	Threshold (MeV)	JP	Decay mode
Ground	—	0+	—
1st excited	5.014	0+	$e^- + e^+$
2nd excited	5.119	3-	$\gamma$
3rd excited	6.148	2+	

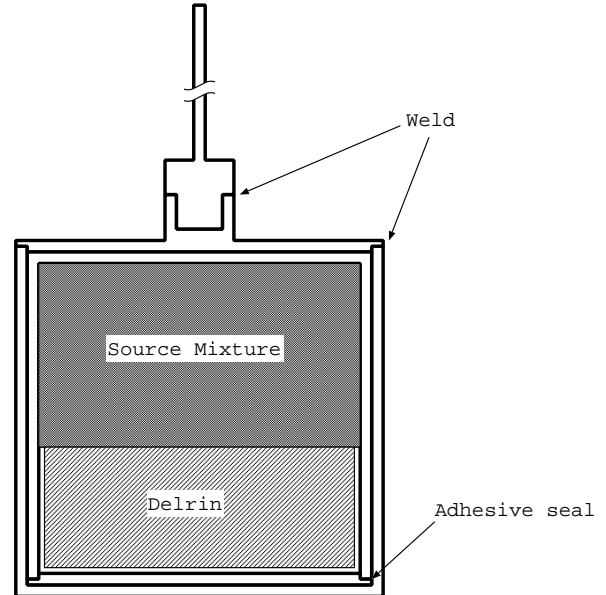


Fig. 1. Construction of the source capsule. The chamber is 13 mm in diameter and 13 mm in height. Both capsules have 1 mm thick walls. The inner capsule was inserted with the lid away from the joint in the outer capsule to protect the adhesive from the heat of welding.

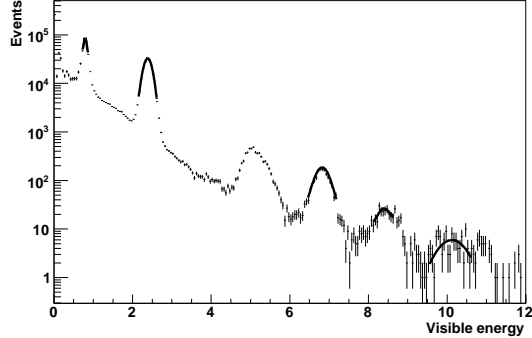


Fig. 2. Reconstructed singles energy spectrum. The spectrum has been corrected to allow for dead-time below NSUM of 190. The fits are (left to right) the 803 keV gamma, the neutron capture on hydrogen, the 6.13 MeV gamma from the second excited state of  $^{16}\text{O}$ , and two background complexes from neutron capture on Fe, Ni, and Co. The unfit peak at 5 MeV includes both neutron capture on carbon and neutron inelastic scattering on carbon. The 1022 keV peak is too small to be visible on this plot. The continuum is largely the response of the LS to fast neutrons. The energy scale of the plot is linear in collected charge and calibrated to the 2.2 MeV neutron capture peak.

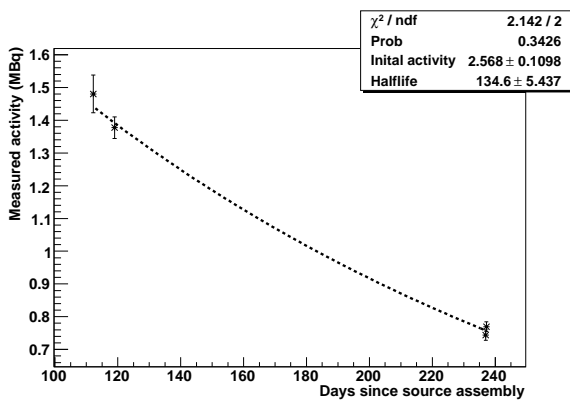


Fig. 3. Contained  $^{210}\text{Po}$  activity of the source as measured in KamLAND. Activity is computed from the area of a Gaussian fit to the peak at 803 keV, and is not corrected for scattering losses in the source capsule.

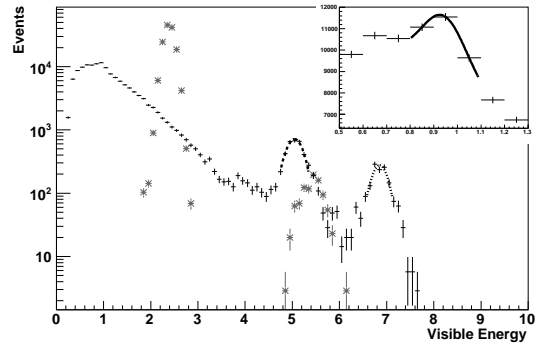


Fig. 4. Reconstructed coincidence energy spectra. Plotted are both the prompt (black points) and delayed (gray asterisks) energy spectra. The insert shows an expanded view of the prompt spectrum in the region of the 1022 keV line. The lines are fits to the positron annihilation peak (solid), the carbon inelastic peak (dashed), and the 6.13 MeV gamma events from the second excited state (dotted). The coincidence selection algorithm applies cuts on the delayed event energy, so no continuum is present between the hydrogen and carbon capture peaks.